water

MDPI

Article

Responses of Baseflow to Ecological Construction and Climate Change in Different Geomorphological Types in The Middle Yellow River, China

Qiannan Yang, Zhanbin Li, Yong Han and Haidong Gao *

State Key Laboratory of Eco-Hydraulics in Northwest Arid Region of China, Xi'an University of Technology, Xi'an 710048, Shaanxi, China; hyangqn2016@163.com (Q.Y.); zhanbinli@126.com (Z.L.); hanyong2006@163.com (Y.H.)

* Correspondence: hdgao@msn.cn; Tel./Fax: +86-29-8231-2658

Received: 13 December 2019; Accepted: 15 January 2020; Published: 20 January 2020

Abstract: Baseflow is a critical component of streamflow in arid areas. Determining variations in baseflow and the factors affecting it have positive roles for water resource utilization in arid watersheds. Two watersheds, the Hailiutu River watershed (HLTR) and the Dali River watershed (DLR), located in two different geomorphological regions of the middle Yellow River, were selected for this study. By using the Eckhardt segment method (fourth digital filtering method, DF4), baseflow was separated from streamflow based on its daily data. Mann-Kendall trend test analysis (M-K trend test) was used to test the trends in baseflow change at different times. Complex Morlet wavelet analysis was used to judge baseflow periodicity. Heuristic segmentation and sequential cluster analysis were used to identify the potential change points in the baseflow series for the two regions together with Pearson correlation coefficient. The results showed: (1) the annual baseflow of the HLTR and the DLR showed significantly decreasing trends ($P < 0.01$), more significantly for the HLTR (0.33×10^8 m^3) than the DLR (0.20×10^8 m^3). The annual base flow index (BFI, baseflow/total streamflow) in the wind-sand region (0.75) was larger than for the loess region (0.55), and the BFI in the wind-sand region was more stable in different periods. (2) The annual baseflow of the HLTR and the DLR both exhibited a complete main cycle of 42 years and 38 years, respectively. The change points of the annual baseflow in the HLTR were 1967 and 1986, and 1971 and 1996 in the DLR. (3) There was no significant change in annual precipitation in the two watersheds, while annual reference evapotranspiration (ET_0) in the DLR showed a significant increasing trend ($P < 0.01$). The normalized difference vegetation index (NDVI) on the DLR (0.40) was higher than on the HLTR (0.26). (4) Baseflow in the wind-sand region, where vegetation improvement was the only ecological activity, decreased faster than in the loess region where there had been numerous ecological measures such as vegetation improvement, check dams and terraces. This implied that comprehensive measures such as these were helpful in slowing the rate at which the baseflow decreases. Therefore, the effect of ecological construction should be considered in future baseflow studies in other geomorphological types within the Middle Yellow River Basin.

Keywords: The Middle Yellow River; baseflow; human activity; climate change

1. Introduction

Baseflow is an important component of streamflow in arid and semi-arid areas, and plays a crucial role in maintaining production and domestic water supply and the health of the watershed ecosystem [1]. Aggravated by climate change and human activity on the land, water resource problems in watershed areas become increasingly serious [2]. More attention is being focused on the

change of baseflow and what influences it (climate, underlying surface conditions and hydrological characteristics) [3–5].

Previous studies of the factors influencing baseflow have mainly concentrated on two aspects: the geological and climatic characteristics of the watershed [6]. Mwakalila et al. calculated the BFI for a semi-arid area in Tanzania, and used regression analysis to reveal the influence of watershed features on the baseflow. He believed that the correlations between BFI, climate and geological conditions in the watershed were significant, being characterized by high precipitation and low evapotranspiration, and a rich granite or basalt underlying surface. From analysis of hundreds of watersheds in Australia, Lacey and Grayson considered that the correlation between BFI and underlying surface (geological/vegetation combination) was not significant [7]. Using Pearson correlation and stepwise multiple regression, Sandhi et al. analyzed the relationships between topography, precipitation, potential evapotranspiration, sediment concentration and baseflow, and showed that topography, sediment concentration and BFI were closely related, whereas topography (river slope), precipitation and baseflow were not significantly related [8]. Arnell considered that the two most basic meteorological factors, precipitation and temperature, have direct impacts on the baseflow of a watershed [9], but Schaake and Liu tended to believe that streamflow in low-flow periods was more affected by climate change than in flood periods [10]. Wilby et al. used a large-scale hydrological model to simulate the relationship between climate change and watershed baseflow, and the results showed that the baseflow was most affected by climate change in wet seasons, but was most affected by land use in dry seasons [11]. Arnell analyzed the frequency of extreme floods in Europe, and found that droughts and elevated temperatures were not a direct cause of decreased baseflow [12].

With the development of a regional social economy, the contradiction between supply and demand of water resources in the middle reaches of the Yellow River have become increasingly prominent, and there is an urgent need to determine the influences of climate change and human activities on the evolution of watershed baseflow. In recent years, the study of streamflow in the region has mainly focused on water and sediment change [13–15]. For each of the geomorphological types in the region, the responses of baseflow to climate change and human activities are different. There is still a lack of research, especially on the characteristics of baseflow change and its influencing factors. Wang et al. analyzed the temporal and spatial evolution relationships and the driving factors of baseflow in the Yellow River in Basin in the past 50 years [16]. They showed that the baseflow in the middle reaches of the Yellow River have decreased significantly in that time. Yang et al. analyzed the factors influencing baseflow change in the Wuding River Watershed, and considered that the greatest influences were check dams and instances of returning farmland to forest or grassland [17]. Lei et al. used the Kuye River Watershed as the research object to explore the driving factors of watershed baseflow change. They thought that, although the change in precipitation was a factor to some extent, the main driving factors were the large-scale exploitation of coal resources and the over-exploitation of groundwater in the watershed [18].

However, yet there has been insufficient local research on the effect of ecological engineering measures on baseflow, especially check dams and terraces. As a key measure for the control of soil and water loss in the Loess Plateau, check dams and terraces effectively block sediment flow from slope to gully and also control gully erosion and flooding, and improve the utilization of water resources in small watersheds [14].

Therefore, the main objectives of the present study were to examine, for different geomorphological land types: (1) the changing trends and cyclical differences in baseflow, and identify the change points; (2) the influence of rainfall and evaporation on baseflow; and (3) the effects of different types and intensity of ecological construction on the rate of change of baseflow in the watershed.

2. Data and Methods

2.1. Study Area

The HLTR and the DLR, located in the middle reaches of Yellow River, were selected as the research objects. Both of these serve the primary tributaries of the Wuding River (Figure 1), which is the largest tributary of the Yellow River.

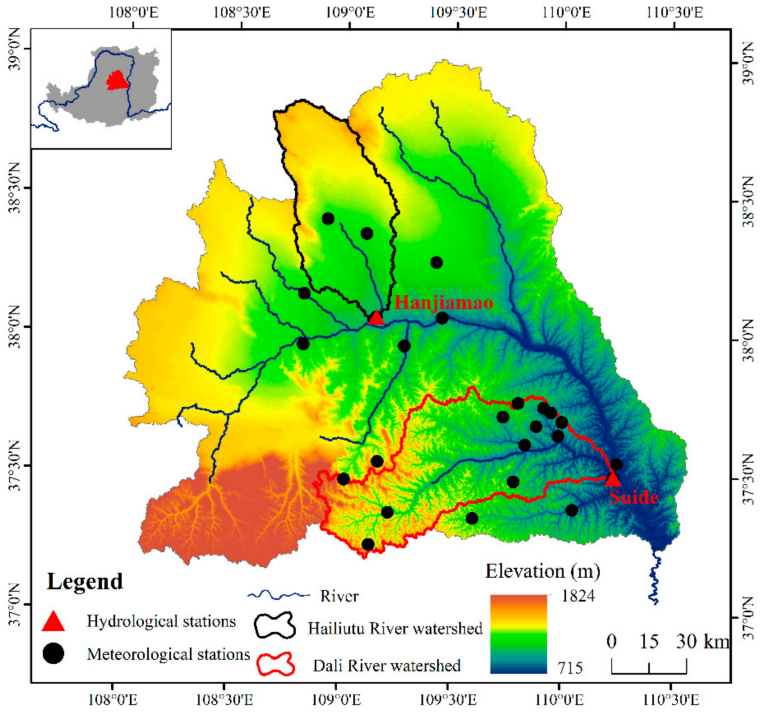

Figure 1. Location of Hailiutu River watershed and Dalihe River watershed.

The HLTR (38°06′–38°50′ N, 108°37′–109°15′ E) is a wind-sand landform. The total length of the river is 85 km, the drainage area is 2645 km^2, the average gradient of the river is 3.36‰, and the average gradient of the watershed is 5 degrees. The HLTR has a semi-arid continental climate in the middle-temperate zone. The average annual precipitation is 445 mm, mostly in short duration, high intensity rainfall. The precipitation from June to October accounts for more than 75 percent of annual precipitation. The average ET_0 is 1225 mm. The soil in the watershed is mostly highly permeable wind-driven sand conducive to rainfall infiltration. The vegetation is mainly composed of Artemisia sphaeroides, Salix, Caragana and Seabuckthorn.

The DLR is a loess hill-gully landform (37°30′–37°56′ N, 109°14′–110°13′ E). The total length of the river is 159.9 km, the drainage area is 3904 km^2, the average gradient of the river is 3.16‰, and the average gradient of the watershed is 17 degrees. The climate of the watershed is warm temperate semi-arid continental monsoon, with 537 mm annual average precipitation, 78 percent of which falls from June to October. The rainfall mostly occurs in the form of short duration, high intensity rainstorms. The annual average ET_0 is 1200 mm. The soil type is mainly loess, and the land-use type is mainly cultivated land, grassland and forest [19].

2.2. Data Sources

Daily streamflow and precipitation data are recorded in the hydrological yearbook of the Yellow River Basin. Data for the HLTR is recorded for the years 1957–2015, and 1960–2015 for the DLR. Daily meteorological data are from the China meteorological data-sharing network, includes seven rainfall stations and one meteorological station in the HLTR, and 16 rainfall stations and one meteorological

station in the DLR. The ET_0 was calculated by the Penman formula which combines daily mean temperature, wind speed, air pressure and solar radiation [20].

The data for check dams was taken from the 2011 National Water Conservancy Census in which the survey indicators included time of completion, coordinates, control area, total storage capacity and silt storage capacity of large check dams. The data for terraces was from the monitoring center of the soil and water conservation of Yellow River, obtained by visual interpretation of remote sensing satellite images from the Gaofen-1 satellite. NDVI data is from the MOD13Q1 NDVI data set in the National Aeronautics and Space Administration (NASA) EOS/MODIS data product (available on https://ladsweb.modaps.eosdis.nasa.gov) for the period 1981–2015 (time resolution 16 days, spatial resolution 8 km). The annual NDVI value was obtained by the maximum value synthesis method.

2.3. Methodology

2.3.1. Baseflow Segment Method

Digital Filtering (DF) is widely used to calculate continuous baseflow quickly and effectively. The DF4 method proposed by Eckhardt was used to segment baseflow [21], obtained from

$$b_t = \frac{\alpha(1 - B_{\max})b_{t-1} + (1 - \alpha)B_{\max}Q_t}{1 - \alpha B_{\max}} \quad (1)$$

where b_t and b_{t-1} are the baseflow amount at times t and $t - 1$ (m^3/s); Q_t is streamflow rate at time t (m^3/s); $b_t \leq Q_t$; α is a filtering coefficient in the general value range 0 to 1; t is the time (days); and $B_{\max}$ is the maximum baseflow coefficient of the river. In this study, $B_{\max} = 0.5$.

2.3.2. Periodic Analysis of Baseflow

Complex Morlet wavelet analysis was used to analyze the adopted periods. This method achieves a good balance between time and frequency, and eliminates spurious oscillations generated by real wavelet transform coefficients, and has no orthogonality. The basic function formula of the complex Morlet wavelet is

$$\varphi_0(t) = \frac{1}{\sqrt{\pi f_b}} \exp\left[-\frac{t^2}{f_b} + (2\pi f_c t)i\right] \quad (2)$$

where f_b is the wavelet bandwidth; f_c is the wavelet center frequency; and $i = \sqrt{-1}$. To facilitate the change of the wavelet scale and the real scale, usually $f_c = 1$.

The cross-wavelet transform (XWT) has been used to examine the way in which watershed hydrological elements change over different time scales, and to find any correlation that may exist between hydrological elements and the influencing factors over different time periods [22].

The XWT principle may be summarized as follows. The wavelet transform from cross-spectrum analysis generates a new signal spectrum, which in effect analyzes the degree of correlation between two time series and thus shows the relationship between any two-time scales within the time-frequency domain. The XWT between two time series $x(t)$ and $y(t)$ is given by

$$W_{xy}(a, \tau) = C_x(a, \tau)C_y^*(a, \tau) \quad (3)$$

where $C_x(a, \tau)$ is the wavelet transform coefficient of $x(t)$; $C_y^*(a, \tau)$ is the complex conjugate of the sequence $y(t)$ wavelet transform coefficient.

2.3.3. Change Point of Baseflow Identification

Heuristic segmentation and sequential clustering were used to distinguish the point at which an annual baseflow series changes. Heuristic segmentation is effective when dealing with nonlinear and non-stationary time series [23]. Based on the t-test, non-stationary time series were segmented into

multiple stable time series with different mean values, overcoming the disadvantages in previous test methods for detecting non-stationary time series. In the segmentation process, multiple iterations were halved to reduce the number of calculations. The minimum sequence size required by the algorithm is 25.

Sequential clustering analysis estimates the most likely change point in a hydrological time series by statistical analysis, then carries out a specific analysis for the actual situation. The main idea of segmentation is to minimize the sum of the squares of dispersions between classes [24].

Assuming that the possible change point is τ, the sum of the squares of the deviations before and after the change point are respectively:

$$V_\tau = \sum_{i=1}^{\tau} (x_i - \overline{x}_\tau)^2,\ V_{n-\tau} = \sum_{i=\tau+1}^{\tau} (x_i - \overline{x}_{n-\tau})^2 \quad (4)$$

where $\overline{x}_\tau$, $\overline{x}_{n-\tau}$ are the average values of the two parts of τ.

The sum of the total squared deviations is given by

$$S_n(\tau) = V_\tau + V_{n-\tau} \quad (5)$$

when $S = \min\{S_n(\tau)\}(2 \le \tau \le n-1)$, τ is the most likely change point.

The Mann-Kendall (M-K) test was adopted using SPSS22.0 software (IBM, New York, USA) to find the significance of trends in precipitation, streamflow and baseflow sequences.

3. Results

3.1. Baseflow Trend Test on an Annual Scale

Table 1 showed that the annual average baseflow amount of the HLTR was 0.62×10^8 m^3 and the annual average BFI was 0.75 for the period 1957–2015. For the DLR over the same period, the annual average baseflow was 0.69×10^8 m^3 and the annual average BFI was 0.55.

Table 1. Statistical characteristics of hydrological indicators in watersheds of different geomorphic types.

Statistical Indicators	HLTR			DLR		
	Annual Streamflow Amount /10^8 m^3	Annual Baseflow Amount /10^8 m^3	BFI	Annual Streamflow Amount /10^8 m^3	Annual Baseflow Amount /10^8 m^3	BFI
Minimum value	0.42	0.33	0.59	0.38	0.27	0.38
Maximum value	1.61	1.15	0.80	2.62	1.15	0.72
Average value	0.83	0.62	0.75	1.33	0.69	0.55
Variation coefficient	0.24	0.24	0.06	0.37	0.26	1.48

The annual baseflow of the HLTR was less than for the DLR, but the BFI was higher. Furthermore, the variation coefficient (C_V) of the annual average baseflow amount in the HLTR and DLR showed middle-degree variation, and their C_V values were similar (0.24 for HLTR; 0.26 for DLR). However, the C_V values for the BFI in the two watersheds were significantly different (0.06 for HLTR, indicating weak variation; up to 1.48 for DLR), implying a more stable annual baseflow and annual streamflow in the HLTR.

The M-K trend test indicated that the annual baseflow decreased significantly for both the HLTR ($Z = -5.32$) and DLR ($Z = -3.16$) throughout the period studied ($P < 0.01$). The annual BFI showed a decreasing trend in the HLTR ($Z = -0.16$) and an increasing trend in the DLR ($Z = 1.53$), but neither trend was significant.

3.2. Annual Baseflow Amount Cycle Change

One main period was found in the annual baseflow of both watersheds (Figure 2). The baseflow cycle of the HLTR was 42 years (Figure 2a). On this time scale, the annual baseflow indicated a high→low→high pattern: 1957–1972 was the high value stage, 1978–1992 was the low value stage, and a high-value stage after 2000.

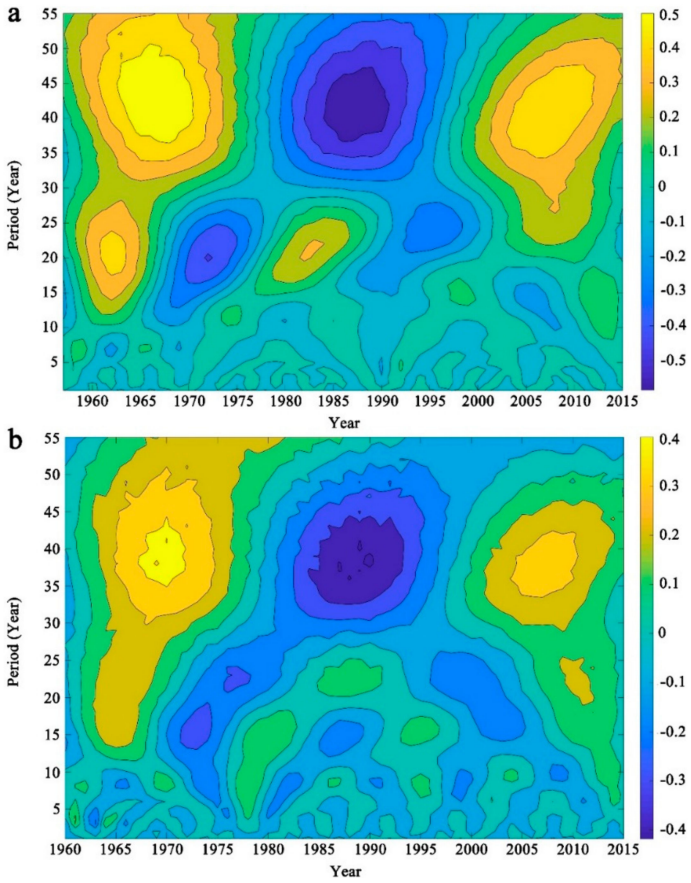

Figure 2. The baseflow real part map of wavelet coefficients of two watersheds. (**a**). Hailiutuhe; (**b**). Dalihe

The baseflow cycle of the DLR was 38 years (Figure 2b). On this time scale, the annual baseflow also showed a high→low→high pattern: high 1960–1975, low 1980–1995, and a high value stage after 2000.

3.3. Change Points in Annual Baseflow Amount

The change points in annual baseflow amount by heuristic segmentation were 1968 and 1986 for the HLTR, and 1996 for the DLR (Figure 3). Sequential clustering indicated change points in 1967 and 1986 for the HLTR, and 1971 and 1996 for the DLR. Thus, both approaches produced similar results. Combined with previously reported results [25], in the present study it was concluded that there were two baseflow change points in the DLR, namely 1971 and 1996.

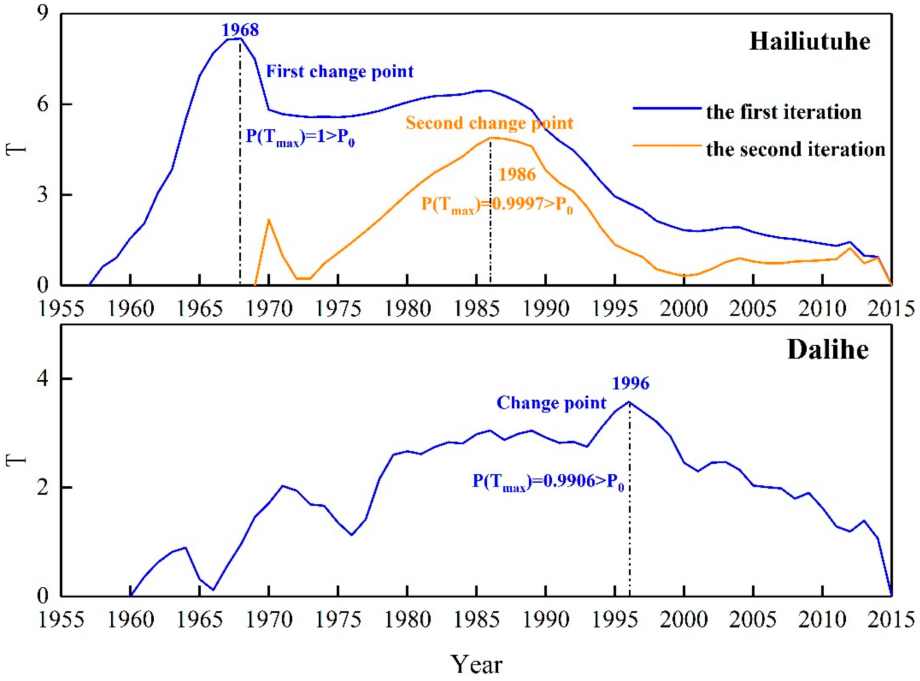

Figure 3. Cumulative anomaly curve of annual baseflow in two watersheds.

Accordingly, the hydrological sequences of both watersheds were divided into three stages: HLTR, 1957–1967, 1968–1986 and 1987–2015; and DLR, 1960–1971, 1972–1996 and 1997–2015. Despite differences in the high-low annual baseflow amount of the two watersheds (Figure 2), the periodicity was relatively synchronous with the change points.

3.4. Baseflow Amount Difference in Different Geomorphic Types

Combined with previous research [26,27], the actual governance processes of the two watersheds was totally different. As discussed above, three periods were defined.

In the DLR during the first period 1960–1971 (the basic period, DLR_P1), the underlying surface was close to its natural condition. 1972–1996 was an engineering construction period (DLR_P2), when water and soil erosion control on the watershed were developed rapidly, especially in the number of check dams and terraces. 1997–2015 was a period of continual vegetation improvement (DLR_P3).

In the HLTR, 1957 to 1967 is considered to be basic period (HLTR_P1); however, no construction has been carried out on the watershed since 1968, but vegetation had been gradually improved. To compare the two areas, the hydrological sequence of the HLTR from 1968 to 2015 was divided into two periods: 1968–1986 was the initial stage of vegetation improvement (HLTR _P2 period), and from 1987 to 2015 was the vegetation construction period (HLTR _P3 period).

The changes in annual baseflow amount and annual BFI of the two watersheds in the three periods are listed in Table 2. The baseflow amount of the DLR was not stable in all three periods. The annual baseflow amount of the HLTR decreased from 0.85×10^8 m^3 in the HLTR_P1 to 0.52×10^8 m^3 in the HLTR _P3, a decrease of 0.33×10^8 m^3. The DLR baseflow amount decreased from 0.78×10^8 m^3 in the DLR_P1 to 0.58×10^8 m^3 in the DLR_P3, a decrease of 0.20×10^8 m^3. Although there was a greater baseflow amount in HLTR_P1 than in DLR_P1, after more than 50 years of treatment, it was lower than the DLR_P3 baseflow amount in the third period.

Table 2. Variation characteristics of two watersheds' baseflow amount during three periods.

Watershed	Period	Baseflow Amount/10^8 m^3		BFI	
		Average Value	Variation Coefficient	Average Value	Variation Coefficient
HLTR	HLT_P1	0.85	0.15	0.77	0.04
	HLT_P2	0.64	0.11	0.75	0.06
	HLT_P3	0.52	0.16	0.75	0.07
DLR	DLH_P1	0.78	0.30	0.70	0.10
	DLH_P2	0.73	0.23	0.74	0.06
	DLH_P3	0.58	0.18	0.73	0.09

The BFI of HLTR decreased slightly and the HLTR_P2 was equal to the HLTR_P3, indicating that the decreasing trend of streamflow was similar to the baseflow amount trend during these two periods. However, although the BFI of the DLR increased from DLR_P1 to DLR_P2, it was basically flat during DLR_P3. This indicated that after DLR_P2, streamflow decreased more rapidly than baseflow.

There were no engineering works in HLTR but it is evident that, in both watersheds, the condition of the underlying surface changed significantly during the three periods. Therefore, in this study the baseflow amount in the latter of the three periods was selected for determining the baseflow in the previous period, to reveal how changes in the underlying surface conditions affected the baseflow of the HLTR in different periods. Based on the above assumptions, three periods were chosen for comparison: P2–P1, P3–P2 and P3–P1.

It can be seen in Table 3 that the rate of baseflow changes in the two watersheds were negative in different periods, and that the change was greater in the HLTR than in the DLR. This suggested that the ecological structure in the middle reaches of the Yellow River reduced the amount of baseflow in the DLR watershed. Compared with P3–P1, the rate of change in the baseflow amount was faster in the wind-sand region (with only the single structure) than in the loess region. This suggested that comprehensive improvements helped to slow the rate of decrease in baseflow amount.

Table 3. Comparative changes in annual baseflow amount of two watersheds in different periods.

Indicators	P2-P1		P3-P2		P3-P1	
	HLTR	DLR	HLTR	DLR	HLTR	DLR
Change amount (10^8 m^3)	−0.22	−0.05	−0.12	−0.15	−0.33	−0.20
Change rate (%)	−25.3%	−6.4%	−18.08%	−20.5%	−38.78%	−25.6%

Note: A positive value indicates an increase in baseflow and a negative value indicates a decrease in baseflow.

4. Discussion

4.1. Responses of Baseflow to Climate and Vegetation Change

A number of factors affect the baseflow in a watershed, the most important being change of climate and change of vegetation. Climate factors include precipitation and evapotranspiration. Precipitation, whose changes impact water resources more obviously on a longer time scale, is an important input to the water balance in a watershed [28]. Evapotranspiration is the main water flux of surface runoff. Five to ten percent of conventional precipitation forms runoff into surface water bodies. Some is stored in the soil [29], and the rest is lost as evapotranspiration, accelerating the consumption of water resources [30]. Studies in some areas have shown that increased vegetation coverage reduces surface runoff [31,32]. Based on this, the present study explored the effects of precipitation, evapotranspiration and vegetation changes on watershed baseflow in the two geomorphological types.

First, the M-K trend tests on precipitation and related evapotranspiration showed that the annual precipitation (Z = 1.54) and evapotranspiration (Z = 0.83) in the HLTR and the annual precipitation in

the DLR (Z = 1.15) did not change significantly during the study, but the annual evapotranspiration (Z = 3.21, $P < 0.01$) clearly increased in the DLR.

Furthermore, XWT was used to judge the extent of the influence of precipitation and related evapotranspiration on watershed baseflow. The energy spectrum indicated two resonance cycles in the annual HLTR precipitation and baseflow. The length of the first main cycle was 1–4 years between 1962 and 1970; the second cycle was 2–4 years from 1986 to 1990. The two periods were both at 95% confidence level (Figure 4a). In both periods, annual precipitation change lagged behind baseflow changes, and they were positively correlated.

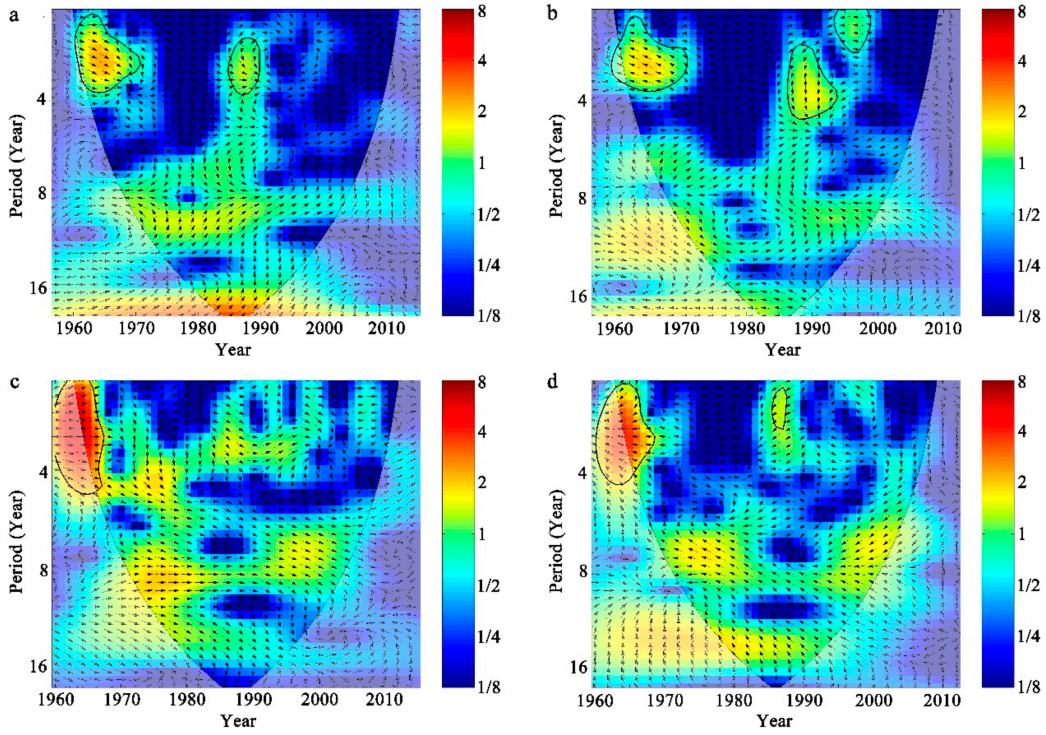

Figure 4. The cross wavelet transforms between precipitation and baseflow series in two watersheds: (**a**) is the Hailiutu River watershed (HLTR), (**b**) is the Dali River watershed (DLR); the cross wavelet transforms between reference evapotranspiration and baseflow series in two watersheds: (**c**) is the HLTR, (**d**) is the DLR.

In the DLR, a resonance cycle was found between annual precipitation and baseflow of 1–5 years between 1962 and 1967, again at 95% confidence level. The annual precipitation change was basically synchronous with baseflow change, and they were positively correlated (Figure 4c).

Three resonance periods were found in the evapotranspiration and annual baseflow in the HLTR (Figure 4b). The evapotranspiration change was in advance of annual baseflow change in the first period of 1–4 years between 1962 and 1972, but lagged behind annual baseflow change in both the second period (2–5 years, 1986–1994) and the third period (1–2 years, 1993–1999). Annual evapotranspiration was negatively correlated with annual baseflow ($P < 0.05$).

In the loess region, two resonance cycles were evident in annual evapotranspiration and annual baseflow in the DLR (Figure 4d). In the first resonance period of 0–5 years from 1964 to 1969, evapotranspiration showed a statistically significant negative correlation with annual baseflow at the 95% confidence level. In the second period of 1–2 years between 1985 and 1987 they were positively correlated ($P < 0.05$), with annual evapotranspiration change lagging behind annual baseflow change.

Figure 5 showed that from 1981 to 2015, the NDVI in both the HLTR and DLR showed a significant increasing trend ($P < 0.001$), but its value was higher in the DLR loess region (0.40) than in the HLTR wind-sand region (0.26). It is evident that the vegetation conditions in both watersheds continued to

improve following many years of restoration, and that the pace of vegetation improvement in the loess region (0.0051) has been more rapid than in the wind-sand region (0.0022). However, the change trend calculations showed that the baseflow in both watersheds decreased with improvement of vegetation conditions, especially in the loess region ($P < 0.01$).

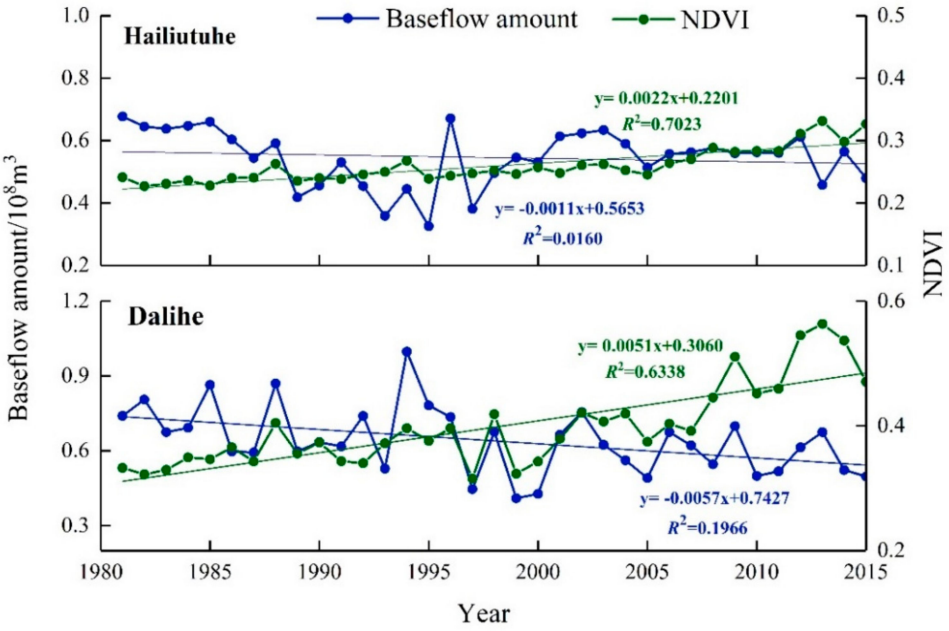

Figure 5. Variation trend of Baseflow amount and normalized difference vegetation index (NDVI) for two watersheds.

Over the whole period covered by the study, neither the precipitation nor the evapotranspiration in either watershed showed any obvious change, but the annual evapotranspiration increased significantly ($P < 0.01$). Baseflow showed higher significant negative correlation with evapotranspiration and C_V in the loess region than in the wind-sand region, indicating that evapotranspiration had a greater impact on baseflow in the loess region, mainly due to the better condition of the vegetation.

The severe evapotranspiration caused by vegetation has considerable influence on the water balance in the watershed [33]. Canopy interception and evaporation both increase with improved vegetation conditions and directly lead to an increase in actual evapotranspiration in the watershed [34,35]. Vegetation increases the streamflow time and extends the concentration of the flow slope to the river, hence increasing both evapotranspiration from land and water [36]. Although vegetation increases groundwater volume by improving the water storage capacity of the soil to a certain extent [37], evapotranspiration due to vegetation is actually about 10 times the intercepted amount of water stored [38].

Although precipitation might increase baseflow, a significant positive correlation existed between precipitation and baseflow only during the reference period in the HTLR, whereas in the DLR the significant positive correlation existed at every stage (Table 4). This showed that in the early reference period, precipitation had a greater impact on baseflow in the wind-sand region, but then its impact decreased after ecological conservation. As for the DLR, water consumption by transpiration increased as the vegetation conditions improved, and the resulting impact on streamflow became increasingly significant. This was the reason for the strong variation of BFI in the DLR watershed. Similar research has confirmed that vegetation in arid and semi-arid areas is more effective in reducing streamflow than in other climatic regions [39], especially in the hill and gully areas of the Loess Plateau [40].

Table 4. Correlation between annual amount of baseflow, precipitation and reference vapotranspiration in different periods in two watersheds.

HLTR			DLR		
Period	**Precipitation**	**ET_0**	**Period**	**Precipitation**	**ET_0**
HLTR_P1	0.368 **	0.008	DLH_P1	0.498 **	−0.349
HLTR_P2	0.464	0.168	DLH_P2	0.746 **	−0.365
HLTR_P3	0.062	−0.337	DLH_P3	0.503 **	−0.403
1957–2015	0.261	−0.356 **	1960–2015	0.552 **	−0.507 **

** Correlation is significant at the 99% level.

4.2. Responses of Baseflow to the Construction of Check Dams and Terraces

A large number of engineering structures such as check dams and terraces have been built in the DLR in the loess region, whereas there are no such structures in the wind-sand region of the HLTR. Therefore, the following discussion of the impact of engineering activity on baseflow is restricted to the DLR.

Since the ecological construction works undertaken in the early 1970s, the number of check dams and the silt storage capacity has risen rapidly. By 2011, 2.78 million check dams had been built, and the silt storage capacity had topped 249.409 million m^3. Pearson correlation analysis (Table 5) showed that the annual baseflow was significantly negatively correlated with silt storage capacity ($R = -0.375$, $P < 0.01$). The silt storage capacity also demonstrated a significantly increasing tendency in each time period ($P < 0.001$), because it reflected the construction speed of the check dams in the watershed. Therefore, as large-scale check dams were being built, they played an increasingly significant role in reducing sediment and water flow. A significant negative correlation between baseflow and silt storage capacity was also noted after the change-point (1972–2011) ($R = -0.373$, $P < 0.05$). Studies have provided evidence that check dams intercept and store local rainfall runoff, and increase soil infiltration and soil-water storage in dam fields [41].

Table 5. Variation trend of silted storage capacity and its correlation with baseflow and base flow index (BFI) in Dali River Basin in different periods.

Time Series	Trend Test		Correlation	
	Silted Storage Capacity	**BFI**	**With Annual Baseflow Amount**	**With BFI**
1960–1971	4.46 ***	−1.17	0.294	−0.440
1972–1996	6.98 ***	−2.27 *	0.038	−0.559 **
1997–2011	5.15 ***	2.94 **	0.142	0.581 *
1972–2011	9.08 ***	0.56	−0.373 *	0.011
1960–2011	10.98 ***	−0.29	−0.375 **	−0.168

* Correlation is significant at the 95% level; ** Correlation is significant at the 99% level; *** Correlation is significant at the 99.99% level.

There were three remarkably distinct periods in the growth rate of the terraced area in the DLR: slowest before 1972, increased between 1972 and 1996, and then remained stable between 1997 to 2011 (Table 6). The M-K trend test demonstrated that the terraced area showed a highly significant increasing trend ($P < 0.001$) and a significantly negative correlation with baseflow throughout the study ($R = -0.397$, $P < 0.01$), with a marked negative correlation with baseflow between 1972 and 2011 ($R = -0.399$, $P < 0.01$). As the terraced area expands, baseflow decreases in the DLR.

Table 6. Change trend of terrace area in Dali River Basin in different periods and its correlation with annual baseflow amount and BFI.

Time Series	Trend Test		Correlation	
	Terraced Area	BFI	With Annual Baseflow Amount	With BFI
1960–1971	4.46 ***	−1.17	0.263	−0.422
1972–1996	6.94 ***	−2.27 *	0.000	−0.631 **
1997–2015	4.83 ***	2.94 **	0.154	0.611 **
1972–2015	9.21 ***	0.56	−0.399 **	−0.04
1960–2015	10.64 ***	−0.29	−0.397 **	−0.19

* Correlation is significant at the 95% level; ** Correlation is significant at the 99% level; *** Correlation is significant at the 99.99% level.

Studies have also shown that terraces reduce streamflow from slopes into rivers [42,43], thus affecting watershed baseflow as distinct from streamflow. This is consistent with findings of an investigation by Li Juan in the Weihe River Watershed of the Loess Plateau [44]. Therefore, it is possible that the baseflow of the watershed decreases with the increasing silt storage capacity and terraced area.

It can be seen from the above analysis that factors other than precipitation led to a decrease in the baseflow. However, of the four factors, precipitation and evapotranspiration remained basically unchanged; therefore, the decreased baseflow evident in the watershed indicated that ecological conservation measures (re-vegetation, check dams, terraces, etc.) had an increasingly significant impact on baseflow. In the HLTR, which has only vegetation and low precipitation, the change rate of baseflow was higher than in the DLR (Table 3). This highlighted the significant impact that vegetation change had on the baseflow in the study area. A study by Ning et al. expressed the view that the remarkable impact of increased vegetation coverage, check dams and terraces on runoff directly causes the reduction in watershed baseflow [45]. The reason for this is that part of rainfall-runoff retained in terraces and check dams returns to the atmosphere due to evaporation, and part of it infiltrates into loess soil [46]. In addition, almost all terraces and dam lands on the Loess Plateau plant crops [47], and large-scale conversion of farmland to forest and grass implemented in this area [48]. However, since the study area is located in semi-arid zone that the evaporation is far greater than precipitation, crops always in a state of water deficit during growth period, so they must absorb soil water to meet their own growth needs. Therefore, the part of water infiltrated into soil still being consumed for vegetation growth [49]. After decades of ecological works, the contribution of the underlying surface conditions has changed in the Loess Plateau and the reduction in runoff and baseflow has tended to be strengthened [31,50].

5. Conclusions

Baseflow is an important ecological factor in arid areas. It is important to analyze the effect of climate change and ecological improvements on baseflow, and to optimize the arrangement of water resources in arid areas. In this study, the baseflow of two watersheds in the middle reaches of the Yellow River (the windsand region of the river (the HLTR) and the DLR, the loess region of the river) were analyzed.

The annual baseflow of each region showed significantly decreasing trends ($P < 0.01$). The BFI of the HLTR (0.75) was larger and less stable than in the loess region (0.55). The annual baseflow of both the HLTR and the DLR were found to be cyclical (42-year and 38-year cycles, respectively).

The baseflow values of both watersheds showed high→low→high periodic change. Heuristic segmentation and sequential clustering analyses found that the change points of the annual baseflows were 1967 and 1986 in the HLTR, and 1971 and 1996 in the DLR. The cycle periods were basically consistent with change points. Due to the differences in ecological improvement measures that had taken place within the cycle periods, the baseflow in the two watersheds was also different. The annual precipitation did not change significantly in either watershed; the ET_0 of the DLR, with its superior

vegetation conditions, increased significantly ($P < 0.01$). Overall, the reduction in HLTR baseflow was more significant than in the DLR, related to the particular geological and geomorphological conditions of the watersheds, together with the hydrological cycle process and the increased use of irrigation water for farmland. The baseflow of the two geomorphological types was decreasing, which is more evidence of the important effect of ecological conditions on watershed baseflow. However, the baseflow in the wind-sand region, where the only activity had been to improve the vegetation, decreased more rapidly than in the loess region with various ecological improvements (vegetation, check dams and terraces).

Although improvements to vegetation and the construction of check dams and terraces has led to a reduction in baseflow in the watershed, the overall impact of the various measures will help to slow the rate of decline of the baseflow. Therefore, further ecological construction on the Loess Plateau should follow the principles of zonality and adaptation to local conditions, and pay attention to the overall planning of the river watershed, strengthen the comprehensive ecological management, give full play to the natural restoration capacity of the Loess Plateau, and do what is necessary to protect water resources and improve the ecological environment of the Loess Plateau in the new era.

Author Contributions: Q.Y. and H.G. conceived the main idea of the paper. Z.L. and Y.H. designed and performed the experiment. Q.Y. wrote the manuscript and all authors contributed in improving the paper. All authors have read and agreed to the published version of the manuscript.

Funding: This research was supported by the National Key Research and Development Program (2016YFC0402406) and the National Natural Science Foundation of China (NO. 41877077).

Acknowledgments: We thank the reviewers for their useful comments and suggestions.

Conflicts of Interest: The authors declare no conflict of interest

References

1. Lin, X.Y.; Liao, Z.S.; Qian, Y.P.; Su, X.S. Baseflow separation for groundwater study in the Yellow River basin. *China. J. Jilin Univ. (Earth Sci. Edition)* **2009**, *39*, 959–967.
2. Piao, S.L.; Ciais, P.; Huang, Y.; Shen, Z.H.; Peng, S.S.; Li, J.S.; Zhou, L.P.; Liu, H.Y.; Ma, Y.C.; Ding, Y.H.; et al. The impacts of climate change on water resourcesand agriculture in China. *Nature.* **2010**, *467*, 43–51. [CrossRef] [PubMed]
3. Stednick, J.D. Monitoring the effects of timber harvest on annual water yield. *J. Hydrol.* **1996**, *176*, 79–95. [CrossRef]
4. Bronstert, A.; Niehof, D.; Bilrger, G. Effects of climate and land-use change on storm runoff generation: Present knowledge and modeling capabilities. *Hydrol. Process.* **2002**, *16*, 509–529. [CrossRef]
5. Tallaksen, L. A review of baseflow recession analysis. *J. Hydrol.* **1995**, *165*, 349–370. [CrossRef]
6. Mwakalila, J.; Feyen, J.; Wyseure, G. The influence of physical catchment properties on baseflow in semi-arid environments. *J. Arid Environ.* **2002**, *52*, 245–258. [CrossRef]
7. Lacey, G.C.; Grayson, R.B. Relating baseflow to catchment properties in south-eastern Australia. *J. Hydrol.* **1998**, *204*, 231–250. [CrossRef]
8. Santhi, C.; Allen, P.M.; Muttiah, R.S.; Arnold, J.G.; Tuppad, P. Regional estimation of base flow for the conterminous United States by hydrologic landscape regions. *J. Hydrol.* **2008**, *351*, 139–153. [CrossRef]
9. Arnell, N.W. Factors controlling the effects of climate change on river flow regimes in a humid temperate environment. *J. Hydrol.* **1992**, *132*, 321–342. [CrossRef]
10. Schaake, J.C.; Liu, C.Z. Development and application of simple water balance models to understand the relationship between climate and water resources. In *New Directions for Surface Water Modeling, Proceedings of the Baltimore Symposium, Baltimore, MD, USA, 2–4 May 1989*; IAHS Publication: Wallingford, UK, 1989; pp. 343–352.
11. Wilby, R.; Greenfield, B.; Glenny, C. A coupled synoptic-hydrological model for climate change impact assessment. *J. Hydrol.* **1994**, *153*, 265–290. [CrossRef]
12. Arnell, N.W. Changing frequency of extreme hydrological events in northern and western Europe. *FRIENDS Hydrol.* **1989**, *187*, 237–249.

13. Gao, Z.L.; Fu, Y.L.; Li, Y.H.; Liu, J.X.; Chen, N.; Zhang, X.P. Trends of streamflow, sediment load and their dynamic relation for the catchments in the middle reaches of the Yellow River over the past five decades. *Hydrol. Earth Syst. Sci.* **2012**, *16*, 3219–3231. [CrossRef]
14. Hu, C.H.; Zhang, X.M. Several key questions in the researches of runoff and sediment changes and trend predictions in the Yellow River. *J. Hydraul. Eng.* **2018**, *49*, 1028–1039.
15. Gu, C.J.; Mu, X.M.; Gao, P.; Zhao, G.J.; Sun, W.Y. Changes in run-off and sediment load in the three parts of the Yellow River basin, in response to climate change and human activities. *Hydrol. Process.* **2019**, *33*, 585–601. [CrossRef]
16. Wang, Y.L.; Wang, W.K.; Qian, Y.P.; Duan, L.; Yang, Z.Y. Change characteristics and driving forces of baseflow of Yellow River basin. *J. Nat. Resour.* **2008**, *23*, 479–486.
17. Yang, Q.N.; Li, Z.B.; Lu, K.X.; Gao, H.D.; Wang, J. Base flow variation characteristics and reason analysis of arid region river: A case study of Wuding River basin. *Taiwan Water Conserv.* **2019**, *66*, 67–75.
18. Lei, Y.N.; Zhang, X.P.; Zhang, J.J.; Liu, E.J. Change trends and driving factors of base flow in Kuye River catchment. *Acta Ecol. Sinica* **2013**, *33*, 1559–1568.
19. Li, B.B.; Li, Z.B.; Hao, Z.Y.; Yang, S.L.; Huang, J.X. Response of vegetation pattern characteristics to sediment yield in Dali River basin. *Trans. the Chin. Soc. Agric. Eng.* **2017**, *33*, 171–178.
20. Valiantzas, J.D. Simplified limited data Penman's ET0 formulas adapted for humid locations. *J. Hydrol.* **2015**, *524*, 701–707. [CrossRef]
21. Eckhardt, K. A comparison of baseflow indices, which were calculated with seven different baseflow separation methods. *J. Hydrol.* **2008**, *352*, 168–173. [CrossRef]
22. Qin, Y.; Tang, B.; Wang, J. Higher-density dyadic wavelet transform and its application. *Mech. Syst. Signal Process.* **2010**, *24*, 823–834. [CrossRef]
23. Bernaola-Galván, P.; Ivanov, P.C.; Nunes, A.; Luís, A.; Eugene, S.H. Scale Invariance in the Nonstationarity of Human Heart Rate. *Phys. Rev. Lett.* **2001**, *87*, 168105. [CrossRef] [PubMed]
24. Wang, W.S.; Jin, J.L.; Ding, J. *Stochastic Hydrology*, 3rd ed.; Chinese Water & Power Press: Beijing, China, 2016.
25. Ren, Z.P.; Ma, Y.Y.; Wang, Y.S.; Xie, M.Y.; Li, P. Runoff changes and attribution analysis in tributaries of different geomorphic regions in Wuding River under ecological construction. *Acta Ecol. Sin.* **2019**, *39*, 4309–4318.
26. Mu, X.M.; Zhang, L.; McVicar, T.R. Estimating the Impact of Conservation Measures on Stream-flow Regime in Catchments of the Loess Plateau, China. *Hydrol. Process.* **2007**, *21*, 2124–2134.
27. Dou, L.; Huang, M.B.; Hong, Y. Statistical Assessment of the Impact of Conservation Measures on Streamflow Responses in a Watershed of the Loess Plateau. *Water Resour. Manag. China* **2009**, *23*, 1935–1949. [CrossRef]
28. Vörösmarty, C.J.; Green, P.; Salisbury, J. Global water resources: Vulnerability from climate change and population growth. *Science* **2000**, *289*, 284–288. [CrossRef]
29. Swank, W.T.; Crossley, D.A., Jr. *Forest Hydrology and Ecology at Coweeta*; Springer: New York, NY, USA, 1988.
30. Jaramillo, F.; Destouni, G. Local flow regulation and irrigation raise global human waterconsumption and footprint. *Science* **2015**, *350*, 1248–1251. [CrossRef]
31. Feng, A.Q.; Li, Y.Z.; Gao, J.B.; Wu, S.H.; Feng, A.X. The determinants of streamflow variability and variation in Three River Source of China: Climate change of ecological restoration? *Environ. Earth Sci.* **2017**, *76*, 1–10. [CrossRef]
32. Guzha, A.C.; Rufino, M.C.; Okoth, S.; Jacobs, S.; Nobrega, R.L.B. Impacts of land use and land cover change on surface runoff, discharge and low flows: Evidence from East Africa. *J. Hydrol. Reg. Stud.* **2018**, *15*, 49–67. [CrossRef]
33. Jin, X.M.; Guo, R.H.; Zhang, Q.; Zhou, Y.X.; Zhang, D.R.; Yang, Z. Response of vegetation pattern to different landform and water-table depth in Hailiutu River basin, Northwestern China. *Environ. Earth Sci.* **2014**, *71*, 4889–4898. [CrossRef]
34. Seeger, M. Uncertainty of factors determining runoff and erosion processes as quantified by rainfall simulations. *Catena* **2007**, *71*, 56–67. [CrossRef]
35. Lotfalian, M.; Parsakhoo, A.; Kavian, A.; Hosseini, S.A. Runoff and sediment concentration of different parts of a road in Hyrcanian forests. *Forest Ecosyst.* **2013**, *15*, 144–151. [CrossRef]
36. Peel, M.C.; Mcmahon, T.A.; Finlayson, B.L. Vegetation impact on mean annual evapotranspiration at a global catchment scale. *Water Resour. Res.* **2010**, *46*, 2095–2170. [CrossRef]

37. Zhang, L.; Dawes, W.R.; Walker, G.R. Response of mean annual evapotranspiration to vegetation change sat catchment scale. *Water Resour. Res.* **2001**, *37*, 701–708. [CrossRef]
38. Xia, L.; Song, X.Y.; Fu, N.; Cui, S.Y.; Li, L.J.; Li, H.Y.; Li, Y.L. Effects of forest litter cover on hydrological response of hillslopes in the Loess Plateau of China. *Catena* **2019**, *181*, 1–11. [CrossRef]
39. Wang, L.X.; Xu, Z.Q. Advances in the Study of Ecohydrological Effects from Vegetation Changes. *World Forestry Res.* **1998**, *6*, 15–24.
40. Mu, X.M.; Xu, X.X.; Wang, W.L. The impact of high-level controlling of soil and water loss on watershed rundff in the Loess Plateau. *J. Arid Land Resour. Environ.* **1998**, *4*, 120–127.
41. Jiang, D.S. *Soil Erosion and Control Models in The Loess Plateau*; China Water & Power Press: Beijing, China, 1997.
42. Shao, H.; Baffaut, C.; Gao, J.E. Development and application of algorithms for simulating terraces within SWAT. *Trans. ASABE* **2013**, *56*, 1715–1730.
43. Zhang, X.P.; Zhang, L.; Mu, X.M.; Li, R. The mean annual water balance in the Hekou-Longmen section of the Middle Yellow River: Testing of the regional scale water valance model and its calibration. *Acta Geogr. Sin.* **2007**, *7*, 753–763.
44. Li, J.; Gao, J.E.; Zhang, Y.X.; Shao, H. Effects of terrace on runoff and ecological base flow of Jinghe Watered in Loess Plateau region. *Bull. Soil Water Conserv.* **2015**, *35*, 106–116.
45. Ning, T.T.; Li, Z.; Liu, W.Z. Separating the impacts of climate change and land surface alteration on runoff reduction in the Jing River catchment of China. *Catena* **2016**, *147*, 80–86. [CrossRef]
46. Jiang, C.; Zhang, H.Y.; Wang, X.C.; Feng, Y.Q.; Labzovskii, L. Challenging the land degradation in China's Loess Plateau: Benefits, limitations, sustainability, and adaptive strategies of soil and water conservation. *Ecol. Eng.* **2019**, *127*, 135–150. [CrossRef]
47. Liu, G.B. Soil conservation and sustainable agriculture on the Loess Plateau: Challenges and prospects. *Ambio* **1999**, *28*, 663–668.
48. Feng, X.M.; Fu, B.J.; Piao, S.L.; Wang, S.; Ciais, P.; Zeng, Z.Z.; Lu, Y.H.; Zeng, Y.; Li, Y.; Jiang, X.H. Revegetation in China's Loess Plateau is approaching sustainable water resource limits. *Nat. Clim. Chang.* **2016**, *6*, 1019–1022. [CrossRef]
49. Jing, K.; Zheng, F.L. Effects of soil and water conservation on surface water resource on the Loess Plateau. *Res. Soil Water Conserv.* **2004**, *04*, 13–14+75.
50. Yang, D.W.; Shao, W.W.; Yeh Pat, J.-F.; Yang, H.B.; Kanac, S.; Oki, T. Impact of vegetation coverage on regional water balance in the nonhumid regions of China. *Water Resour. Res.* **2009**, *45*, 1–13. [CrossRef]